Equation consistency in electron-only reconnection manuscripts

Taylor Kalin
https://taylorkalin.com ; teylersf@gmail.com
ORCID: https://orcid.org/0009-0003-9000-9315
Version 1.0.0; 29 October 2026

Abstract

We check the equations in Liu et al.'s arXiv:2407.06020v2, its publisher-hosted accepted manuscript, and the supplement embedded in that arXiv version. The inspected main system has a continuity sign and a dimensional pressure coefficient inconsistent with its stated Appendix rewrite. After restoring the pressure coefficient, the printed continuity sign gives growing rather than oscillatory linear modes. Separately, the supplemental density-energy term lacks the one-half coefficient required by its claimed quadratic invariant. An exact periodic state demonstrates nonconservation of that printed sum while the consistently weighted sum is conserved. Direct Gaussian projection also gives collisionless Hermite streaming and forcing signs opposite to those printed in the supplied hierarchy. These repairs reconcile the displays with the established KREHM equations; they do not introduce a new plasma model. The source's reconnection-rate and conditional coalescence scalings retain their algebraic support. The subscription version of record and final journal supplement were not obtained, and no conclusion about the actual solver or numerical curves follows from these consistency tests.

1. Editions and purpose

Liu, Silva, Milanese, Zhou, Mandell and Loureiro study electron-only reconnection and inverse magnetic-energy transfer [1]. We read the complete supplied 19-page arXiv:2407.06020v2, including its ten appended supplemental pages, and the authentic ten-page CHORUS accepted manuscript openly linked by APS. The latter contains a cover and nine manuscript pages dated 19 March 2025. It retains the main governing displays and Appendix considered here, while correcting a Figure 1 decimal, consolidating supplement references and changing pagination. The supplied file is byte-identical to official arXiv v2, posted 10 March and dated 11 March 2025.

The associated journal article is Physical Review Letters 134, 155201, DOI 10.1103/PhysRevLett.134.155201. Its subscription version of record was not obtained. The accepted manuscript is a distinct edition; its cover does not establish identity with the typeset article. Supplemental findings below concern specifically arXiv v2, whose supplement is absent from the accepted-manuscript file. We therefore make an edition-specific consistency claim, not a claim that these defects remain in the uninspected journal copies.

The distinctions matter. Appendix A already contains a core sign and coefficient consistent with the original KREHM framework [2]. Its reconnection calculation uses magnitudes and can remain valid despite transcription defects in earlier displays. Our contribution is to document the internal differences and supply reproducible identities that a literal implementation can check. The standard model, energy and Hermite representation belong to the cited prior theory [2,3].

2. Main system and its Appendix reduction

Use the stated positive elementary charge and conventions

$$N = \frac{\delta n_e}{n_0}, \qquad D_t = \partial_t + \frac{c}{B_0}\{\varphi, \cdot\},$$
$$\mathcal{D}_\parallel = \partial_z - \frac{1}{B_0}\{A, \cdot\}, \qquad u = \frac{e d_e^2}{c m_e}\Delta_\perp A. \tag{1}$$

where $\{f, g\} = f_x g_y - f_y g_x$, $A = A_z = A_\parallel$, and $d_e^2 = c^2 m_e/(4\pi n_0 e^2)$. The main article's Eqs. (1) and (2) are on arXiv page 1 and accepted-manuscript printed page 1, PDF page 2. The coefficient-consistent, isothermal, collisionless system is

$$D_t N = -\mathcal{D}_\parallel u,$$
$$D_t(A - d_e^2 \Delta_\perp A) = -c\partial_z \varphi + \frac{c T_e}{e}\mathcal{D}_\parallel N. \tag{2}$$

KREHM Eqs. (39) and (40) give these signs and the pressure coefficient under the same conventions [2]. The inspected main Eq. (1) instead prints a positive parallel derivative of u, and its Eq. (2) omits cT_e/e in front of the density gradient. A bare ∇N has inverse-length dimensions; it cannot be added to $\partial_t A$ in the dimensional notation being used. An explicitly declared normalization could set a coefficient to one numerically, but would have to transform the other factors and the claimed Appendix rewrite consistently.

For $\partial_z = 0$, Eq. (2) gives

$$\partial_t N + \frac{c}{B_0}\{\varphi, N\} = \frac{e d_e^2}{c m_e B_0}\{A, \Delta_\perp A\}. \tag{3}$$

This is the positive bracket printed in Appendix (A1), arXiv page 5 and accepted-manuscript PDF page 6. Direct reduction of the printed positive main parallel derivative instead gives a negative bracket. Changing $A_\parallel$ to $-A_z$ cannot repair this quadratic term because $\{-A, \Delta(-A)\} = \{A, \Delta A\}$. Appendix (A2) also restores the missing pressure coefficient. A positive parallel derivative does occur in KREHM summary Eq. (62), but there it evolves a polarization variable equal to minus the density perturbation [2]. That change of dependent variable must be retained.

The linear check isolates the sign after restoring the pressure units. For a perpendicular Fourier symbol $0 \le \Gamma_0 < 1$, Poisson closure gives $\varphi = -T_i N/[e(1 - \Gamma_0)]$. About a uniform guide field, the consistently signed pair has

$$\omega^2 = \frac{k_\parallel^2 d_e^2 k_\perp^2}{m_e(1 + d_e^2 k_\perp^2)}\left(T_e + \frac{T_i}{1 - \Gamma_0}\right) > 0. \tag{4}$$

The printed continuity sign gives the opposite frequency squared, equivalently positive real time-growth eigenvalues. Figure 1 illustrates the isolated contrast. It is not an instability observed in the source's simulation. A plausible explanation is that the implementation uses the established equations while the displays contain transcription defects.

3. The density coefficient in the energy invariant

Supplement Eq. (12), supplemental page 8 or combined arXiv page 17, prints $Y_\mathrm{p} = n_0 T_e \langle N^2 \rangle$ and writes $U + K_i + K_e + Y_\mathrm{p}$ as a conserved free energy. Its other terms retain their usual coefficients. Let brackets denote a periodic volume mean. In the strict-subion closure $\varphi = -T_i N/e$, the consistent terms are

$$
\begin{aligned}
U &= \frac{\langle|\nabla_\perp A|^2\rangle}{8\pi}, \qquad K_e = \frac{d_e^2\langle(\Delta_\perp A)^2\rangle}{8\pi}, \\
K_i &= \frac{n_0 T_i}{2}\langle N^2\rangle, \quad Y_{1/2} = \frac{n_0 T_e}{2}\langle N^2\rangle.
\end{aligned}
\tag{5}
$$

The one-half density coefficient is also explicit in KREHM Eqs. (70)–(71) [2]. We interpret the source's finite-FLR ion term in its usual self-adjoint quadratic-form sense, not as an operator acting on an already squared field. In the subion limit its printed definitions imply $K_i/Y_{\rm p} = T_i/(2T_e)$. At equal temperatures this is one half, whereas the following supplemental explanation invokes $K_i \approx Y$. The consistent density coefficient yields $K_i/Y_{1/2} = T_i/T_e$.

Conservation supplies a stronger test than that ratio. For the two-dimensional periodic Appendix system ($\partial_z = 0$), write $F = A - d_e^2\Delta A$, $\alpha = ed_e^2/(cm_eB_0)$ and $I = \langle N\{A, \Delta A\}\rangle$. Retain the full Appendix advection of F, including its inertial part. Periodic integration by parts then gives

$$
\frac{d(U+K_e)}{dt} = -n_0\alpha(T_i+T_e)I, \qquad \dot{K}_i = n_0\alpha T_i I, \qquad \dot{Y}_{1/2} = n_0\alpha T_e I. \tag{6}
$$

In particular, $\langle\Delta A\{\Delta A, N\}\rangle = 0$ cancels the integrated inertial-advection contribution; the inertial-advection field itself need not vanish. Equation (6) conserves $U + K_e + K_i + Y_{1/2}$, but replacing only $Y_{1/2}$ by $Y_{\rm p} = 2Y_{1/2}$ leaves $n_0\alpha T_e I$. The density variance is not separately invariant for general coupled states, so a change in its diagnostic name cannot repair the unweighted sum.

An exact periodic witness on $[0, 2\pi]^2$ is

$$
\begin{aligned}
A &= \cos x + \cos 2y, \quad N = \sin x \sin 2y, \\
\{A, \Delta A\} &= -6\sin x \sin 2y, \quad I = -\frac{3}{2}.
\end{aligned}
\tag{7}
$$

The unit-amplitude fields specify an algebraic normalization. Scaling both by any $0 < \epsilon < 1$ makes the density $n_0(1+\epsilon N)$ positive and the fluctuations arbitrarily small; I and the nonzero energy residual scale as ϵ^3. Thus the discrepancy does not depend on using order-one density perturbations.

Choose coherent nondimensional coefficients $G = 1$, $\kappa = 1$, $n_0 = \alpha = 1$, $T_e = T_i = 1$, $d_e^2 = 1/4$, where the magnetic energy is $G/2$ times its quadratic form and $G\kappa = n_0\alpha$. Exact inversion of $1 - d_e^2\Delta$ gives

$$
\begin{aligned}
(\dot{U}, \dot{K}_e, \dot{K}_i, \dot{Y}_{1/2}) &= \left(\frac{21}{20}, \frac{39}{20}, -\frac{3}{2}, -\frac{3}{2}\right), \\
\dot{W}_{1/2} = 0, \qquad \dot{W}_{\rm p} &= -\frac{3}{2}.
\end{aligned}
\tag{8}
$$

These are instantaneous derivatives of a synthetic admissible state, not a time integration or a measured heating rate. Figure 8 of the source could already use the consistent coefficient; its raw arrays and implementation were not obtained. Neither that figure nor the order-of-magnitude equipartition assumption is rejected by this test.

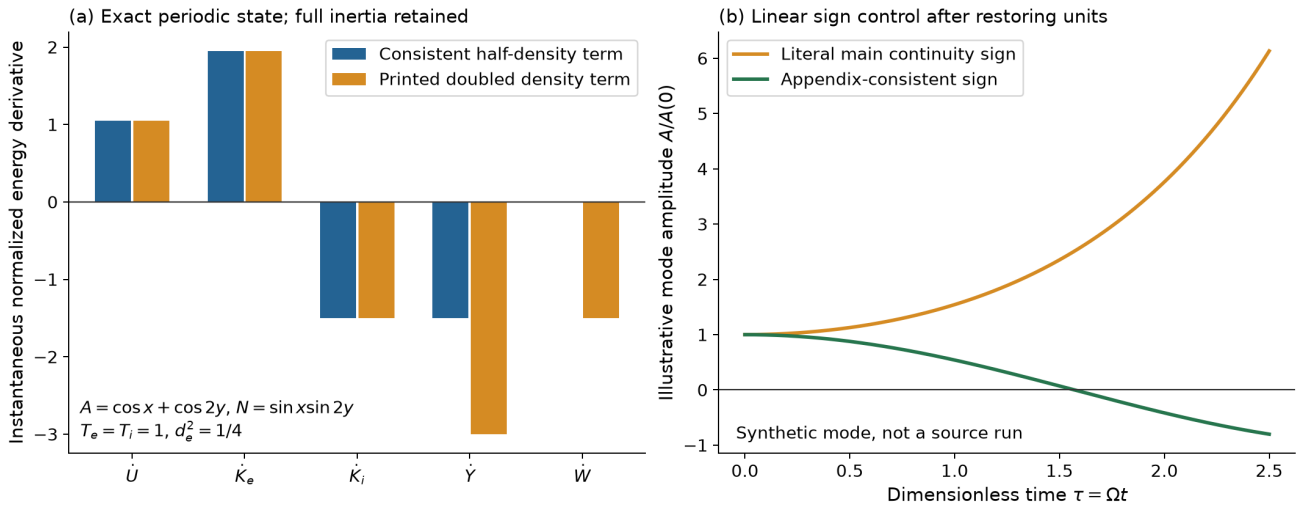


Figure 1. Left: the exact ledger of Eq. (8), retaining full inertia, compared with changing only the density coefficient. Right: the unit-frequency linear control $A/A(0) = \cos\tau$ or $\cosh\tau$ after restoring the pressure coefficient, with initial amplitude one and initial derivative zero. Both panels are synthetic equation checks; neither reproduces a source run.

4. Collisionless Hermite projection

Supplement Eq. (9), combined page 15, uses $F_0 \propto e^{-z^2}$, $z = v_\parallel/v_{\rm the}$, and the expansion $\psi_m = H_m/\sqrt{2^m m!}$. Its drive is $(1-2z^2)F_0\mathcal{D}_\parallel u$. The stated physicists' Hermite convention fixes

$$H_2 = 4z^2 - 2, \qquad 1 - 2z^2 = -\sqrt{2}\,\psi_2, \qquad \langle H_2(1-2z^2)\rangle_{F_0} = -4, \quad \langle H_2^2\rangle_{F_0} = 8. \tag{9}$$

Thus the projected g_2 drive is negative $\sqrt{2}\mathcal{D}_\parallel u$, while supplement Eq. (11) prints a positive sign. In the two-dimensional case used for its non-isothermal experiment, Eq. (9)'s left-hand streaming term is $+v_\parallel\mathcal{D}_\parallel(g - \theta F_0)$, where $\theta = \delta T_{\parallel e}/T_e$. With collisions set to zero, projection gives

$$D_t g_m = -v_{\rm the}\mathcal{D}_\parallel\left(\sqrt{\frac{m+1}{2}}\,g_{m+1} + \sqrt{\frac{m}{2}}\,g_{m-1} - \delta_{m1}g_2\right) - \sqrt{2}\,\delta_{m2}\mathcal{D}_\parallel u, \qquad m \geq 2. \tag{10}$$

The printed hierarchy instead has positive streaming on its right-hand side. KREHM Eq. (93) independently corroborates Eq. (10) [2]. For example, the $g_2 \leftarrow g_3$ coefficient on that side is $-\sqrt{3/2}$ and the temperature moment obeys $D_t\theta + \sqrt{3}v_{\rm the}\mathcal{D}_\parallel g_3 = -2\mathcal{D}_\parallel u$.

Reversing the velocity coordinate rephases odd Hermite coefficients but leaves the even $m = 2$ forcing unchanged. A redefinition that changes this forcing must also change the supplied distribution expansion and temperature moment. These silent changes do not make the two stated equations identical. Figure 2 shows the direct Gaussian identities. We assign no sign to the separately written collision functional; the contradiction already exists without collisions. Reversing a streaming matrix alone also does not establish failed Landau damping in an uninspected implementation.

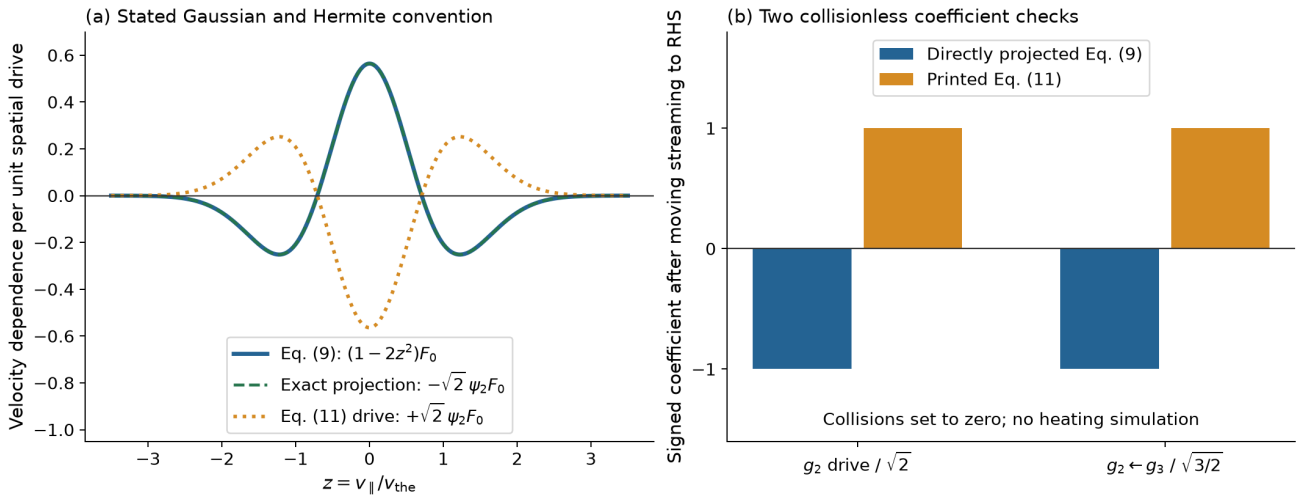


Figure 2. Left: the source in Eq. (9) and its exact negative-$\sqrt{2}$ Hermite representation overlap; the positive representation has the opposite sign. Right: two signed coefficients after moving streaming to the right-hand side. Collisions are zero, and no heating simulation is supplied.

5. Retained physics and additional presentation limits

Using the consistent Appendix coefficients and the source assumptions $\delta_x \sim d_e$, $\delta_y \sim R$ and $A_{\mathrm{sheet}} \sim B_\perp d_e$ retains

$$\tau_{\mathrm{rec}} \sim \frac{R}{d_e}\tau, \qquad \mathcal{R}_{\mathrm{rec}} \sim \sqrt{1 + T_i/T_e}\,\frac{\rho_s}{R}, \qquad \mathcal{R}_{\mathrm{rec},e} \sim \frac{d_e}{R}. \tag{11}$$

The last two rates use different normalizing velocities. Exceeding a familiar ion-Alfvén-normalized value is not by itself an impossible outflow-normalized rate. Conserved island flux $RB_\perp$, volume filling and a merger-controlled lifetime imply $\tau_{\mathrm{rec}} \propto R^2/B_\perp$ and therefore

$$\mathcal{E} \propto t^{-2/3}, \qquad R \propto t^{1/3}, \qquad B_\perp \propto t^{-1/3}, \qquad l \propto t^{2/3} \tag{12}$$

with the source's critical-balance assumption for l. The constant-rate MHD algebra likewise retains $\mathcal{E} \propto t^{-1}$ and $R \propto t^{1/2}$. These are conditional phenomenological deductions; our checks neither refit nor disprove the source's finite-window numerical evidence.

Two subsidiary dimensional displays need clarification. The v2 supplement defines ion beta as $4\pi n_{0i} m_i / B_0^2$, an inverse velocity squared in dimensional Gaussian units. The conventional dimensionless definition is $8\pi n_{0i} T_i / B_0^2$ [3]. Its supplemental Eq. (4) also leaves the combined parallel density derivative without the coefficient $c(T_e + T_i)/e$. These can be documented as presentation inconsistencies without inferring the numerical units used by a solver.

With conventional beta, the supplement's proposed finite-beta rate, with its entire fraction inside the square root, matches the ERMHD coefficient and has the correct common low-beta limit [3]. The source explicitly acknowledges that ideal ERMHD omits flux-breaking physics and labels this extension a hypothesis requiring validation. We retain that admission rather than presenting it as an overlooked defect.

The supplemental length-definition prose reverses the parallel and perpendicular contour-intercept assignments, but the figure axes and reported length scale do not establish that the actual diagnostic was reversed. Overall constants in its normalized structure function and unit local-field direction

cancel and are not additional failures. The supplied shell-advection maps, spectral-peak motion and size growth remain relevant positive observations. Original fields would be needed to remeasure a complete energy-transfer budget.

6. Reproduction, conclusions and availability

The original producer [5] uses full finite Fourier convolution and rational arithmetic, without spectral truncation. For $A = a\cos(mx) + b\cos(ny)$ and $N = h\sin(mx)\sin(ny)$ it checks $I = habmn(m^2 - n^2)/4$. Five patterns $(m, n, a, b, h) = (1, 2, 1, 1, 1), (2, 3, 1/2, 2, -1), (3, 1, 2, 1/3, 3/2), (1, 1, 1, 1, 1), (1, 2, 0, 1, 1)$ cross four $(T_e, T_i) = (1, 1), (1/2, 2), (3, 1/3), (2, 3)$ and three $d_e^2 = 0, 1/4, 2$. These give 60 states, including 24 zero-exchange controls; zero inertia is only a limiting mathematical check. For pattern index $j = 0, \ldots, 4$, $G = 1$, $n_0 = 1 + (j \bmod 2)$, $\kappa = 1/n_0$ and $\alpha = \kappa/n_0$ enforce the required coefficient identity. All 36 nonzero-exchange states distinguish the density weights.

Twenty-four linear-symbol controls cross $\Gamma_0 = 0, 1/4, 3/4$, $(T_e, T_i) = (1, 1), (2, 1/3)$, $d_e^2 = 1/4, 2$ and $k_\perp^2 = 1, 5$, with $k_\parallel^2 = 1/4$ and $m_e = 1/2$. Hermite recurrence constructs H_0 through H_8; exact Gaussian moments verify 81 orthogonality pairs, nine drive projections and six neighboring streaming magnitudes. Separate rate and exponent controls preserve Eqs. (11)–(12). Their eight rational parameter sets are supplemental positive checks, not evidence for a new physical parameter regime. No random sampling, fitted tolerances or source data enter the exact identities. Floating point is used for drawing the two explanatory figures.

The producer's five numerical outputs match across Python 3.12.14 and 3.13.7. Original plots use NumPy 2.3.5 and Matplotlib 3.11.2. Independent implementations and source-bound reading records are preserved separately; none is imported by the producer. Actual runtime receipts, complete parameter tables and artifact hashes accompany the computational package.

GX is an identified public solver framework [4], but no exact target run commit, complete input decks or raw diagnostic arrays were recovered from the inspected manuscript archives. Missing perturbation/seeding information and three-dimensional grid details limit exact transient reproduction; they do not show that the source runs were impossible. We do not replace its simulations with the synthetic controls.

The supported correction concerns the named manuscript equations, their projected hierarchy and their stated invariant. Appendix A and the original KREHM literature already provide the core reconciliation. No different reconnection mechanism, revised numerical curve or new plasma-heating result is established. The final journal VOR and final journal supplement remain outside the verified edition boundary.

Availability: the 55-file computational package is published as software version 1.0.0 at `https://doi.org/10.5281/zenodo.23784871` [5], with public source frozen at commit `83583b1524778b8bb4e5c78482ae7f4f104856cc` in `https://github.com/Teylersf/electron-only-equation-audit` . The complete archive is 393,818 bytes, SHA-256 `d0444c832c21b8a2e60ebd02e576c4ad2077388dfeb9e412590b7049d1e5aabc`. The separately recorded tested Git tree is `7bf82539dd5224ec9328dc94848b2a62dc6b4029`; it is not a commit. The software archive excludes the manuscript and source simulation data. Original code is MIT licensed; original text and figures are CC BY 4.0. Third-party works retain their rights. The software DOI is not evidence of manuscript acceptance.

Funding and disclosures: Taylor Kalin self-funded this work. No outside funding or competing financial interest was reported. AI systems assisted source comparison, mathematical checking, programming and drafting. Independent internal checks and venue AI review are distinct from external human peer review.

References

[1] Z. Liu, C. Silva, L. M. Milanese, M. Zhou, N. R. Mandell and N. F. Loureiro. Electron-Only Magnetic Reconnection and Inverse Magnetic-Energy Transfer at Subion Scales. Physical Review Letters 134, 155201 (2025). https://doi.org/10.1103/PhysRevLett.134.155201 . Inspected editions: https://arxiv.org/abs/2407.06020v2 and publisher CHORUS accepted manuscript https://link.aps.org/accepted/10.1103/PhysRevLett.134.155201 ; supplemental findings refer only to the ten pages embedded in arXiv v2. Subscription VOR not inspected.

[2] A. Zocco and A. A. Schekochihin. Reduced fluid-kinetic equations for low-frequency dynamics, magnetic reconnection, and electron heating in low-beta plasmas. Physics of Plasmas 18, 102309 (2011). https://doi.org/10.1063/1.3628639 . Primary published copy: https://scientific-publications.ukaea.uk/wp-content/uploads/Published/POPVOL18p102309.pdf . Relevant equations and sections were checked; no whole-paper reading claim is made.

[3] A. A. Schekochihin, S. C. Cowley, W. Dorland, G. W. Hammett, G. G. Howes, E. Quataert and T. Tatsuno. Astrophysical gyrokinetics: kinetic and fluid turbulent cascades in magnetized weakly collisional plasmas. Astrophysical Journal Supplement Series 182, 310 (2009). https://doi.org/10.1088/0067-0049/182/1/310 . Relevant beta/ERMHD sections of https://arxiv.org/abs/0704.0044v4 were checked; no whole-paper reading or independent publisher-byte-identity claim is made.

[4] N. R. Mandell et al. GX: a GPU-native gyrokinetic turbulence code for tokamak and stellarator design. Journal of Plasma Physics 90, 905900402 (2024). https://doi.org/10.1017/S0022377824000631 . Primary framework identification and abstract were checked. Public source: https://bitbucket.org/gyrokinetics/gx ; this is not an identification of the target run version.

[5] T. Kalin. Computational evidence for Equation consistency in electron-only reconnection manuscripts. Software version 1.0.0. Zenodo (2026). https://doi.org/10.5281/zenodo.23784871 . Computational commit 83583b1524778b8bb4e5c78482ae7f4f104856cc.